Original Article Clinics in Orthopedic Surgery 2021;13:320-328 • https://doi.org/10.4055/cios20228

Fluorodeoxyglucose Positron-Emission Tomography/Computed Tomography and Magnetic Resonance Imaging for Adverse Local Tissue Reactions near Metal Implants after Total Hip Arthroplasty: A Preliminary Report

Makoto Kimura, MD, Nobuhiro Kaku, MD, Yuta Kubota, MD, Hiroaki Tagomori, MD, Hiroshi Tsumura, MD

Department of Orthopedic Surgery, Faculty of Medicine, Oita University, Yufu, Japan

Background: Plain computed tomography (CT) and magnetic resonance imaging (MRI) are useful for diagnosing adverse local tissue reactions after metal-on-metal total hip arthroplasty (THA), but metal artifacts can hamper radiological assessments near the implants. We sought to clarify the usefulness of 18F-fluorodeoxyglucose positron-emission tomography (18F-FDG-PET) CT and MRI in the periprosthetic region, which is difficult to assess after THA due to metal artifacts.

Methods: We performed preoperative 18F-FDG-PET/CT and 18F-FDG-PET/MRI, as well as plain CT and MRI, in 11 metal-on-metal THA patients who underwent revision surgery.

Results: Most patients showed high FDG uptake in the metal artifact areas and pseudotumors in the 18-F-FDG-PET/CT and 18-F-FDG-PET/MRI scans. Intraoperative intra-articular macroscopic and histopathological intra-articular granulation tissue findings were suggestive of adverse local tissue reaction.

Conclusions: The enhanced uptake in the metal artifact areas seemed to reflect adverse local tissue reaction. Therefore, 18F-FDG-PET/CT and 18-F-FDG-PET/MRI can be useful for the auxiliary diagnosis of adverse local tissue reactions after metal-on-metal THA.

Keywords: *Arthroplasty, Computed tomography, Fluorodeoxyglucose F18, Metal-on-metal joint prostheses, Positron-emission tomography*

Total hip arthroplasty (THA) has become a popular surgical treatment for hip disease; however, it is commonly followed by pain, which is difficult to diagnose as the cause of it is unknown.[1] There are many possible causes of such pain, including infection, loosening of the prosthesis, and iliopsoas tendinitis. Adverse local tissue reaction (ALTR) and pseudotumors after metal-on-metal (MoM) THA can also cause postoperative pain. It has been reported that ALTR can occur not only on MoM bearing surfaces but also when using polyethylene liners.[2]

ALTR has few other characteristic clinical and physical findings, apart from pain, and cannot be revealed by radiography. Plain computed tomography (CT) and magnetic resonance imaging (MRI) are valuable tools in this respect. ALTR is characterized by the production and proliferation of fluid components or necrotic tissue and often appears between the soft tissues around the artificial joint prosthesis. Numerous reports have shown the usefulness

Received September 19, 2020; Revised December 24, 2020; Accepted December 28, 2020
Correspondence to: Nobuhiro Kaku, MD
Department of Orthopedic Surgery, Faculty of Medicine, Oita University, 1-1 Idaigaoka Hasama-machi, Yufu, Oita 879-5593, Japan
Tel: +81-97-586-5872, Fax: +81-97-586-6647
E-mail: nobuhiro@oita-u.ac.jp

of MRI, which has a clearer soft-tissue delineation than CT.[3] MRI is also recommended in the ALTR diagnostic algorithm for MoM THA.[4]

However, even with MRI, which allows diagnosis of pseudotumors away from the metal prosthesis, lesions in the prosthesis' vicinity are difficult to assess due to the influence of metal artifacts. Many studies have reported that metal ions from bearing surfaces and head-neck junctions within the joint can cause ALTR.[5] Therefore, the existence of an abnormality, particularly in the early stages of ALTR, often cannot be determined by imaging, as the initial pathogenesis of ALTR is likely to be in the vicinity of the prosthesis. Improving the diagnostic performance in this metal artifact area is an essential requirement for the early detection of ALTR, even in the absence of a remote pseudotumor or fluid collection. The usefulness of metal-artifact-reduction sequence (MARS)-MRI modalities has been reported in recent years, but they are not yet commonly used.[6]

18F-fluorodeoxyglucose positron-emission tomography (18F-FDG-PET) has been recognized as a useful imaging modality for cancer detection.[7] In addition, its usefulness for detecting post-THA surgical infections and laxity has recently been reported.[8] In recent years, it has become possible to perform 18-F-FDG-PET/CT and 18-F-FDG-PET/MRI in combination with each other, which allows for simultaneous anatomical and qualitative evaluation by PET. CT is usually more versatile because it has a wider imaging area and requires a shorter imaging time. However, when the pathology has a limited location, MRI is more valuable than CT, particularly for anatomical identification of soft tissues and evaluation of fluid lesions, and it does not involve radiation exposure.

The use of 18F-FDG-PET to investigate ALTR after THA has rarely been reported[9-11] and has been limited to 18F-FDG-PET alone or 18F-FDG-PET/CT combination. However, there have been no reports of 18F-FDG-PET combined with MRI. In addition, there are no reports of the usefulness of 18F-FDG-PET/CT and 18F-FDG-PET/MRI in the area where metal artifacts appear near the artificial joint. The purpose of this study was to clarify the usefulness of 18F-FDG-PET/CT and 18F-FDG-PET/MRI for evaluations of the region near the prosthesis with metal artifacts in patients with ALTR after THA.

METHODS

Ethics

This prospective study was performed in accordance with the ethical standards as laid down in the 1964 Declaration of Helsinki and its later amendments or comparable ethical standards. The present study was approved by the Institutional Review Board of Oita University (IRB No. 1396; April 16, 2018), and all study participants provided informed consent before the initiation of FDG-PET.

Patients

The present study included patients with recurrent hip pain after primary MoM THA, who underwent revision surgery between May 2018 and February 2020. ALTR was suspected, and revision surgery was performed because of poor clinical improvement, resistance to conservative treatment, and prolonged or increased pain in all patients. The study population consisted of 9 patients with 11 joints (6 right hips and 5 left hips). Eight patients were female, and 1 was male. The causative diseases were osteoarthritis of the hip in 8 cases and rheumatoid arthritis in 3 cases. The acetabular components used in the primary THA were the M2aMagnum (Biomet, Warsaw, IN, USA) in 6 cases, the M2aRadial (Biomet) in 2 cases, the Pinnacle in 2 cases (DePuy Synthes, Warsaw, IN, USA), and the Metasul in 1 case (Zimmer, Warsaw, IN, USA). For the femoral stem, 2 patients received an AML prosthesis (DePuy Synthes), 1 patient received a Natural Hip stem (Zimmer), and 8 patients received a Bi-Metric stem (Zimmer). A revision was performed using a posterolateral approach, and cementless implants were used in all cases. Eight of the revisions consisted of the liner and ball-head-only replacements, while 3 were acetabular-side revisions. There were no cases of simultaneous bilateral surgery.

After a preoperative MRI, 18F-FDG- PET/MRI was performed to evaluate the area in which metal artifacts occur in the vicinity of the prosthesis. We focused on the presence or absence of FDG uptake around the hip joint, the maximum standardized uptake value (SUV) in the early phase, and the maximum SUV in the delay phase. Imaging diagnoses, including determining whether pseudotumors were present outside the metal artifacts, were performed by two orthopedic surgeons (MK and NK).

Preoperative Plain CT

CT was performed using a Biograph 40 TruePoint (Siemens, Munich, Germany) with a slice thickness of 3 mm and an interval of 2 mm.

Preoperative Plain MRI

Patients underwent MRI with a MAGNETOM Skyra (Siemens), and a 3.0-T MRI scanner was used with T1-weighted spin-echo (SE), T2-weighted SE, and short tau inversion recovery (STIR) sequences.

Acquisition of PET/CT and MRI

According to the FDG-PET protocol, all patients fasted for at least 6 hours before the examination, and the 18F-FDG dose was 3.7 MBq/kg. 18F-FDG-PET images were acquired within the range of the orbit to the thigh using a BIOGRAPH 40 PET scanner (Siemens). The blood sugar levels were checked before the injection, and the scan was performed if blood sugar levels were < 150 mg/dL. The early and delayed phase images were obtained after 60 minutes and between 90 and 120 minutes, respectively. The FDG-PET data were reconstructed in a 168 × 168 matrix.

CT was performed using the same scanner (BIOGRAPH 40; Siemens) at 120 kV and 220 mAs (CARE Dose4D). The slice thickness was 3 mm, and the interval was 2 mm. MRI was performed on a 3-T system (Achieva; Philips, Best, The Netherlands) using a 32-channel cardiac coil. MR images were obtained with T1-weighted, T2-weighted, and STIR sequences in the coronal and axial planes, and diffusion images were also obtained, all of which represent MARS-MRI.

Image Analysis

The 18F-FDG-PET/MRI was reconstructed with image analysis software (AZE Virtual Place Fujin; AZE, Chiyoda, Japan) because the 18F-FDG-PET and MRI devices were independent. The SUVmax was calculated in the area of the highest uptake around the artifact near the artificial joint. In the evaluation of pseudotumors, uptake in the 18F-FDG-PET/MRI was expressed as high uptake (SUV value of 3.5 and above and colored red), highly photopenic (SUV of 1.76 to 3.4 and colored orange or yellow), weak (SUV of 0.1 to 1.75 and colored green), and none (SUV of 0 and colored purple or black).

Histological Review

Resected samples were preserved in 10% buffered formalin, and sections were stained with hematoxylin and eosin by a pathological technologist (MK). Specimens obtained by revision operation were evaluated by a pathologist (MK) and an orthopedic surgeon (NK). Pathology results were calculated using the aseptic lymphocytic-dominated vasculitis-associated lesion (ALVAL) score, based on the report of Campbell et al.[12] The ALVAL score was evaluated based on three factors: synovial lining, inflammatory infiltration, and tissue organization were scored on a scale of 0–3, 0–3, and 0–4 points, respectively, with a total score rated on a 10-point scale. A total score of 0–4 was classified as low, 5–8 as moderate, and 9–10 as high. In cases where the assessments between the two evaluators differed, scores were discussed until a consensus was reached.

RESULTS

The mean age at revision was 68.4 ± 5.9 years. The mean time from primary THA to examination was 7.1 ± 3.9 years, and this period exceeded 3 years in all patients. All patients had dull pain (Table 1). Laboratory data, such as

Table 1. Patient Characteristics

Case no.	Sex	Age* (yr)	Side	Original disease	Acetabular implant model	Stem implant model	Interval period† (mo)	WBC (× 10^3/μL)	CRP (mg/dL)
1	F	70	R	RA	Pinnacle	AML	58	5.2	0.07
2	F	70	L	RA	Pinnacle	AML	55	5.2	0.07
3	M	82	R	OA	Metasul	Natural hip	66	4.6	0.7
4	F	58	L	OA	M2aMagnum	Bi-Metric	42	8.55	1.4
5	F	75	L	OA	M2aMagnum	Bi-Metric	62	6.55	0.11
6	F	66	L	OA	M2aRadial	Bi-Metric	73	5.17	0.08
7	F	66	R	OA	M2aRadial	Bi-Metric	84	9.47	0.12
8	F	68	R	RA	M2aMagnum	Bi-Metric	81	7.84	0.04
9	F	69	R	OA	M2aMagnum	Bi-Metric	95	4.97	0.04
10	F	64	R	OA	M2aMagnum	Bi-Metric	89	4.99	0.06
11	F	65	L	OA	M2aMagnum	Bi-Metric	84	4.86	0.08

WBC: white blood cell count, CRP: C-reactive protein, R: right, L: left, RA: rheumatoid arthritis, OA: osteoarthritis of the hip.
*Age at revision surgery. †The period from primary total hip arthroplasty to the examination.

the white blood cell count and C-reactive protein level, did not suggest infection in any of the patients. Preoperative radiographs and CT did not show periprosthetic radiolucency or osteolysis in any of the patients. Preoperative plain CT and MRI showed metal artifacts in the prosthesis' vicinity in all cases, while pseudotumor images outside the metal artifacts were found in 8 cases. All cases demonstrated 18F-FDG-PET uptake within the metal artifact areas, with mean SUVmax values of 4.98 ± 1.45 and 6.06 ± 2.01 in the early phase and delay phase, respectively (Table 2). The difference between the SUVmax values of the early and delay phases was 1.08 ± 1.05. In the 8 cases with non-artifactual pseudotumor images away from the metal artifact area, 4 cases showed strong uptake, and their plain MR images showed areas of mixed brightness in T1, T2, or both sequences (Table 3).

Intraoperatively, all patients had macroscopic necrotic tissue and fluid uptake in the joint (Table 4). The ALVAL score for histopathology of granulation tissue obtained intraoperatively was moderate in 10 cases and low in 1 case (Table 4). Clinical symptoms, such as preoperative pain, improved after revision in all cases.

Case Presentation

Case 2 is a representative case. Plain CT and MRI did not allow evaluation due to the presence of metal artifacts near the artificial joint, but pseudotumors outside the metal artifacts could be visualized more clearly on plain MRI than on plain CT (Fig. 1A and B). 18F-FDG-PET/CT and 18F-FDG-PET/MRI showed high uptake in the metal artifact area (Fig. 1C and D). As 18F-FDG-PET/MRI provides clearer findings for muscles and pseudotumors surrounding the metal artifact than 18F-FDG-PET/CT, it facilitates

Table 3. Findings of Pseudotumor Outside of Metal Artifacts in Plain MRI and PET/MRI

Case no.	MRI T1	MRI T2	Uptake of PET/MRI
1	NP	NP	NP
2	Low	High	None
3	Mixed	Mixed	High uptake overall
4	Low	High	High uptake overall
5	NP	NP	NP
6	Iso	Mixed	Highly photopenic
7	Low	Mixed	Highly photopenic
8	Low	High	Weak
9	Iso	High	Weak
10	NP	NP	NP
11	Low	High	None

MRI: magnetic resonance imaging, PET: positron-emission tomography, NP: there were no findings of pseudotumor on MRI, Mixed: mixed signal intensity.

Table 2. FDG-PET Images in the Area of Metal Artifacts

Case no.	Uptake of PET/CT and MRI	SUVmax (Early)	SUVmax (Delay)	Difference (SUVmax [delay] – SUVmax [early])
1	Yes	5.897	7.233	1.336
2	Yes	6.197	6.199	0.002
3	Yes	5.051	6.926	1.875
4	Yes	7.555	9.132	1.577
5	Yes	4.649	4.586	–0.063
6	Yes	6.795	10.029	3.234
7	Yes	4.300	5.360	1.06
8	Yes	3.033	3.893	0.86
9	Yes	2.682	3.826	1.144
10	Yes	4.707	3.897	–0.81
11	Yes	3.944	5.609	1.665

FDG-PET: fluorodeoxyglucose positron-emission tomography, CT: computed tomography, MRI: magnetic resonance imaging, SUV: standardized uptake value.

Table 4. Macroscopic and Histological Findings of Intra-articular Tissue

Case no.	Fluid finding*	Necrotic tissue*	ALVAL score			ALVAL total score grading
			Synovial lining	Inflammatory infiltrate	Tissue organization	
1	Bloody, reddish-brown	Yes	3	2	2	Moderate
2	Bloody, reddish-brown	Yes	3	2	2	Moderate
3	Bloody, reddish-brown	Yes	3	1	2	Moderate
4	Cloudy, yellowish	Yes	2	2	3	Moderate
5	Cloudy, yellowish	Yes	2	2	2	Moderate
6	Bloody, reddish-brown	No	2	2	2	Moderate
7	Bloody, reddish-brown	Yes	2	2	2	Moderate
8	Cloudy, yellowish	No	1	2	2	Moderate
9	Bloody, reddish-brown	No	1	2	2	Moderate
10	Cloudy, yellowish	Yes	1	1	2	Low
11	Cloudy, yellowish	Yes	2	2	2	Moderate

ALVAL: aseptic lymphocytic-dominated vasculitis-associated lesion.
*Intra-articular macroscopic findings.

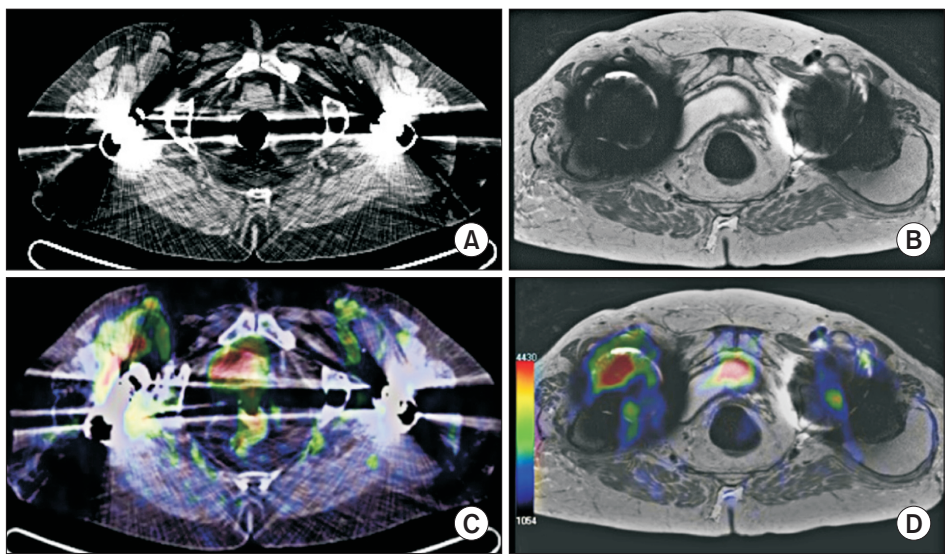

Fig. 1. Preoperative imaging in a 70-year-old female. She underwent bilateral total hip arthroplasty with the same metal-on-metal prosthesis in both hips. (A) Plain computed tomography (CT) image. There are extensive areas around the bilateral hip prostheses that are difficult to assess due to metal artifacts. (B) Plain magnetic resonance imaging (MRI) image (T1). There is a marked artifact on both sides. A cystic pseudotumor is seen posterior to the left hip prosthesis. This can be identified more clearly on MRI than on CT. (C) Fluorodeoxyglucose-positron-emission tomography (FDG-PET)/CT image. Uptake near both prostheses is present in the region of metal artifacts. (D) FDG-PET/MRI image. The large pseudotumor on the left side is clearly visible and no uptake occurred in the area. There are uptakes near the metal implants. The uptakes on PET/MRI are more sharply delineated than on PET/CT. PET/MRI enables the identification of the anatomical positional relationship of uptakes for easier differentiation from the surrounding soft tissue.

the understanding of the anatomical relationship between tissues. Bloody fluid and necrotic tissue were found in the intracapsular joint (Fig. 2A-C), and corrosion of the stem neck or ball head was observed (Fig. 2D and E). The total ALVAL score of this case was 7 (Fig. 2F).

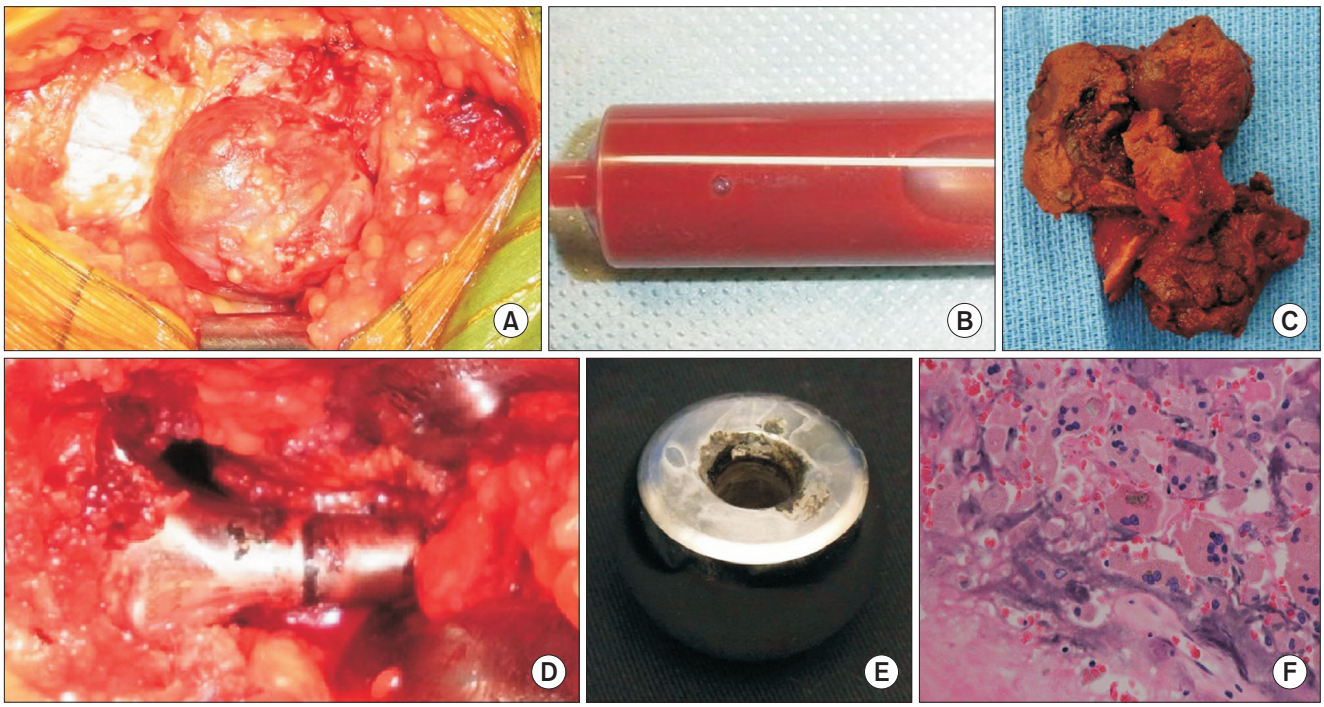

Fig. 2. Intraoperative intra-articular macroscopic findings and histopathological findings of intra-articular granulation tissue. (A) The pseudotumor formation is cystic. (B) Venous joint fluid with a bloody reddish-brown color is present. (C) Necrotic tissue is observed in the intracapsular joint. (D) A portion of the stem neck is discolored and demonstrates macroscopic corrosion. (E) At the fitting portion, the ball head appears to be missing and demonstrates some corrosion. (F) In the joint capsule, giant cells, foam cells, collagen fibers, and metallic powders are present in the tissue. Multinucleated imaginal cell phagocytosis of metallic powder can also be observed (H&E, × 400).

DISCUSSION

In this study, 18F-FDG-PET/CT and MRI were used to evaluate cases of groin pain after MoM THA. 18F- FDG-PET showed high uptake near the prosthesis with metal artifacts on plain CT or MRI in all cases. The enhanced uptake within the metal artifact area seemed to reflect ALTR, indicating that 18F-FDG-PET/CT and 18F-FDG-PET/MRI can be useful for the auxiliary diagnosis of ALTR after MoM THA. The uptakes on 18-F-FDG-PET/MRI were more sharply delineated than on 18-F-FDG-PET/CT, and 18-F-FDG-PET/MRI enabled the identification of the anatomical positional relationship of uptakes for easier differentiation from the surrounding soft tissue.

Groin pain after THA can be caused by various reasons including loosening of the acetabular component, stress fracture, iliopsoas tendinitis, impingement, pelvic osteolysis, and infection, but it can also be caused by ALTR, which is difficult to diagnose based on clinical symptoms alone.[13] If a pseudotumor is present at a distance from the prosthesis, it can be evaluated by CT or MRI. Although a pseudotumor located in an area away from metal artifacts is one of the important findings for the diagnosis of ALTR, there are cases in which a remote pseudotumor has not occurred in the early stages of ALTR. One of our patients had a high uptake in the metal artifact area and no remote pseudotumor in the right hip, and a moderate uptake in the metal artifact area and a large remote pseudotumor without uptake in the left hip (Fig. 1). In this patient, plain MRI could not distinguish ALTR in proximity to the artificial joint because the technique is highly susceptible to interference from metal artifacts. Besides, pseudotumors by ALTR, which can be classified as cystic, solid, and mixed types,[14,15] showed different uptake levels in the present study (Table 3). There was no association between the degree of the uptake in the remote pseudotumor and near the artificial joint in the present study (Tables 2 and 3, Fig. 1). These results also showed that it would be difficult to estimate the degree of inflammation in the artificial joint's vicinity due to ALTR based on findings such as the presence or absence, size, and uptake of a remote pseudotumor. Therefore, it is essential to improve the diagnostic performance of imaging modalities in the metal artifact area in order to allow early detection of ALTR caused by metal ions from the bearing surfaces in the joint and the head-neck junction.

MARS-MRI may be superior to 18F-FDG-PET/MRI in terms of low cost and less invasiveness, avoidance of intravenous administration of 18F-FDG, and radiation exposure. However, even if MARS-MRI leads to a clearer depiction of the metal artifact than plain MRI, it is still unknown whether MARS-MRI can visualize the inflammatory pathology such as ALTR near the artificial joint. Besides, even if dedicated software for MARS is attached to the existing MRI main unit, it will be difficult to reduce artifacts depending on the model of the MRI main unit, and the image of the tissue around metal artifacts will become unclear when the metal artifacts are further reduced by adjusting the sequence.

PET is often used to diagnose neoplasms,[7] and its potential for the assessment of inflammation has been reported. It has been used as a tool for the objective interpretation of the severity of inflammatory diseases, such as rheumatoid arthritis and psoriatic arthritis.[16] The uptake in PET for inflammation has also been characterized as showing less change or a decreasing trend in the application of dual time-point imaging, without showing a markedly increasing trend.[17] Reinartz et al.[8] reported a trend for infection and loosening based on the PET uptake area and SUV uptake values. There are no clear diagnostic cutoffs, although SUVs in cases of infection and loosening have been assessed. Choe et al.[18] found that the mean SUVmax of infection was relatively large at 11 (5–17). Reinartz et al.[8] also stated that for values above 5–6, the possibility of infection may also have to be considered.

Regarding pseudotumors after THA, Kisielinski et al.[9] reported the imaging potential of FDG-PET in a case of removal and revision of a pseudotumor, with an SUVmax of 5 at a distance from the prosthesis. Makis et al. reported that FDG-PET/CT revealed the imaging characteristics of necrotic pseudotumors and differentiated these from malignant soft-tissue tumors.[10] Aro et al. reported the usefulness of 18F-FDG-PET/CT for the imaging of pseudotumors, as compared to 68-Ga citrate.[11] In the present study, the pseudotumor uptake seemed higher for solid or mixed findings on plain MRI (Table 3). On the other hand, Zhuang et al.[19] reported nonspecific and physiological uptakes in contact with the bearing surfaces of the prosthesis and head-neck junction after THA. Gelderman et al.[20] reported a physiological mean SUV of 2.5 at the joint of the prosthesis. Imaging patterns have also been reported for uptake in asymptomatic patients' prostheses.[21] Therefore, caution should be exercised in diagnosing ALTR for all intra-articular uptakes in contact with the prosthesis after MoM THA. Even in moderate uptakes (SUV ≥ 2.5), careful diagnosis using clinical findings is required.

All near-joint uptakes, including those seen in the early and delay phases, had SUVs > 2.5 and showed a marked tendency to accumulate within metal artifact areas rather than in relatively remote pseudotumors. Although malignant lymphomas and gastrointestinal malignancies have been reported to show a tendency to increase the SUV value in the delay phase, as compared to the early phase,[22,23] the mean value in this study was 1.08, without a tendency for a marked increase. The uptake in ALTRs was more pronounced in cases with malignant lymphomas and gastrointestinal malignancies than in pseudotumors in the early phase. On the other hand, there was a variability of SUV values among cases with near-joint uptake (Table 2), although our data showed high SUV values overall. Based on previous reports,[8,18] the SUV value also varies for patients with prosthetic joint infection as an inflammatory disease. It would be especially difficult to determine a definite SUV for the diagnosis of inflammatory diseases. When there seems to be some variability in SUV values in ALTR, it is important not to neglect the comprehensive diagnostic process based on the consideration of other information such as the clinical course of symptoms, blood or joint fluid examinations, and image findings.

18F-FDG-PET features of benign tumors were in contrast to those of malignant tumors. In addition, all cases in this study had macroscopic findings at revision and histopathological findings consistent with ALTR, such as findings of inflammation and necrosis in the joint. Thus, the uptakes seen in PET in the vicinity of the prosthesis after MoM THA may be an imaging finding indicative of ALTR.

Clinical studies showed that it is difficult to diagnose ALTR on plain CT and MRI due to metal artifacts but combining these with 18F-FDG-PET may allow delineation of inflammation (which may cause clinical symptoms, such as pain) in the metal artifact areas. 18-F-FDG-PET/MRI seemed to be superior to 18-F-FDG-PET/CT for understanding the anatomy of the condition because it could better delineate pseudotumors and surrounding soft tissues than 18F-FDG-PET/CT. On the other hand, pseudotumors located away from the joints did not show high uptake, particularly when containing fluid components, demonstrating the limitations of the sensitivity of 18F-FDG-PET examination.

Regarding limitations of the present study, the study design is a case series with a small number of samples, and the time to surgery and the type of scanner used were different in each case. Furthermore, a comparative study with asymptomatic cases was not performed. Although there is no doubt that MRI is safer in terms of radiation exposure

than CT, a previous report[24] has suggested that MRI is problematic in cases with metal prostheses due to thermal fluctuation in the metal, and the choice of using CT is dependent on the patient's preference or condition. MRI and CT should be performed after checking contraindications, such as the possibility of pregnancy, cardiac pacemaker models, and history of claustrophobia. Informed consent should be obtained after a thorough explanation to all patients, including the additional cost.

In conclusion, this study suggests that 18F-FDG-PET/CT and 18F-FDG-PET/MRI could demonstrate the presence of a lesion and the severity of inflammation within metal artifact areas. In addition, 18F-FDG-PET/MRI seems to be excellent for enhancing the understanding of the overall pathology of ALTR after THA, as it also clearly delineates the surrounding soft tissue, including pseudotumors. With imaging study findings in the metal artifact areas using 18F-FDG-PET/CT and 18F-FDG-PET/MRI, we were able to bring ourselves closer to the diagnosis of ALTR based on comprehensive findings, including other information such as the patient's medical history, physical findings, laboratory data, and other image findings. In the present study, we focused on post-THA ALTR, but 18F-FDG-PET/CT and 18F-FDG-PET/MRI should also be useful auxiliary diagnostic tools for the early diagnosis of pathological conditions that develop in the vicinity of the prosthesis after THA, such as iliopsoas tendinitis. However, the diagnosis of post-THA diseases could not be accurately determined with findings of 18F-FDG-PET/CT or 18F-FDG-PET/MRI alone. We hope that our study results will help orthopedic surgeons provide another diagnostic option for patients with unknown pain after THA.

CONFLICT OF INTEREST

No potential conflict of interest relevant to this article was reported.

ACKNOWLEDGEMENTS

We are thankful to Dr. Masashi Kataoka (MD, PhD) for technical support and histological evaluation in the present study. He is the histopathology specialist in the field of orthopedics at Physical Therapy Course of Study, Faculty of Welfare and Health Sciences, Oita University Hospital, Oita, Japan.

ORCID

Makoto Kimura https://orcid.org/0000-0002-7190-6075
Nobuhiro Kaku https://orcid.org/0000-0002-4041-1870
Yuta Kubota https://orcid.org/0000-0003-1426-1482
Hiroaki Tagomori https://orcid.org/0000-0002-6185-0098
Hiroshi Tsumura https://orcid.org/0000-0002-5384-822X

REFERENCES

1. Classen T, Zaps D, Landgraeber S, Li X, Jager M. Assessment and management of chronic pain in patients with stable total hip arthroplasty. Int Orthop. 2013;37(1):1-7.
2. Hjorth MH, Mechlenburg I, Soballe K, Roemer L, Jakobsen SS, Stilling M. Higher prevalence of mixed or solid pseudotumors in metal-on-polyethylene total hip arthroplasty compared with metal-on-metal total hip arthroplasty and resurfacing hip arthroplasty. J Arthroplasty. 2018;33(7):2279-86.
3. Nawabi DH, Gold S, Lyman S, Fields K, Padgett DE, Potter HG. MRI predicts ALVAL and tissue damage in metal-on-metal hip arthroplasty. Clin Orthop Relat Res. 2014;472(2):471-81.
4. Chalmers BP, Perry KI, Taunton MJ, Mabry TM, Abdel MP. Diagnosis of adverse local tissue reactions following metal-on-metal hip arthroplasty. Curr Rev Musculoskelet Med. 2016;9(1):67-74.
5. Natu S, Sidaginamale RP, Gandhi J, Langton DJ, Nargol AV. Adverse reactions to metal debris: histopathological features of periprosthetic soft tissue reactions seen in association with failed metal on metal hip arthroplasties. J Clin Pathol. 2012;65(5):409-18.
6. Jungmann PM, Agten CA, Pfirrmann CW, Sutter R. Advances in MRI around metal. J Magn Reson Imaging. 2017;46(4):972-91.
7. Lee JW, Lee SM. Radiomics in oncological PET/CT: clinical applications. Nucl Med Mol Imaging. 2018;52(3):170-89.
8. Reinartz P, Mumme T, Hermanns B, et al. Radionuclide imaging of the painful hip arthroplasty: positron-emission tomography versus triple-phase bone scanning. J Bone Joint Surg Br. 2005;87(4):465-70.
9. Kisielinski K, Cremerius U, Reinartz P, Niethard FU. Fluordeoxyglucose positron emission tomography detection of inflammatory reactions due to polyethylene wear in total hip arthroplasty. J Arthroplasty. 2003;18(4):528-32.
10. Makis W, Rush C, Abikhzer G. Necrotic pseudotumor caused by a metal-on-metal total hip prosthesis: imaging characteristics on (18)F-FDG PET/CT and correlative imag-

ing. Skeletal Radiol. 2011;40(6):773-7.

11. Aro E, Seppanen M, Makela KT, Luoto P, Roivainen A, Aro HT. PET/CT to detect adverse reactions to metal debris in patients with metal-on-metal hip arthroplasty: an exploratory prospective study. Clin Physiol Funct Imaging. 2018;38(5):847-55.
12. Campbell P, Ebramzadeh E, Nelson S, Takamura K, De Smet K, Amstutz HC. Histological features of pseudotumor-like tissues from metal-on-metal hips. Clin Orthop Relat Res. 2010;468(9):2321-7.
13. Lombardi AV Jr, Barrack RL, Berend KR, Cuckler JM, Jacobs JJ, Mont MA, et al. The Hip Society: algorithmic approach to diagnosis and management of metal-on-metal arthroplasty. J Bone Joint Surg Br. 2012;94(11 Suppl A):14-8.
14. Hart AJ, Satchithananda K, Liddle AD, et al. Pseudotumors in association with well-functioning metal-on-metal hip prostheses: a case-control study using three-dimensional computed tomography and magnetic resonance imaging. J Bone Joint Surg Am. 2012;94(4):317-25.
15. Hauptfleisch J, Pandit H, Grammatopoulos G, Gill HS, Murray DW, Ostlere S. A MRI classification of periprosthetic soft tissue masses (pseudotumours) associated with metal-on-metal resurfacing hip arthroplasty. Skeletal Radiol. 2012;41(2):149-55.
16. Vijayant V, Sarma M, Aurangabadkar H, Bichile L, Basu S. Potential of (18)F-FDG-PET as a valuable adjunct to clinical and response assessment in rheumatoid arthritis and seronegative spondyloarthropathies. World J Radiol. 2012 28;4(12):462-8.
17. Kumar R, Basu S, Torigian D, Anand V, Zhuang H, Alavi A. Role of modern imaging techniques for diagnosis of infection in the era of 18F-fluorodeoxyglucose positron emission tomography. Clin Microbiol Rev. 2008;21(1):209-24.
18. Choe H, Inaba Y, Kobayashi N, et al. Use of 18F-fluoride PET to determine the appropriate tissue sampling region for improved sensitivity of tissue examinations in cases of suspected periprosthetic infection after total hip arthroplasty. Acta Orthop. 2011;82(4):427-32.
19. Zhuang H, Chacko TK, Hickeson M, et al. Persistent nonspecific FDG uptake on PET imaging following hip arthroplasty. Eur J Nucl Med Mol Imaging. 2002;29(10):1328-33.
20. Gelderman SJ, Jutte PC, Boellaard R, et al. 18F-FDG-PET uptake in non-infected total hip prostheses. Acta Orthop. 2018;89(6):634-9.
21. Aydin A, Yu JQ, Zhuang H, Alavi A. Patterns of 18F-FDG PET images in patients with uncomplicated total hip arthroplasty. Hell J Nucl Med. 2015;18(2):93-6.
22. Nakayama M, Okizaki A, Ishitoya S, Sakaguchi M, Sato J, Aburano T. Dual-time-point F-18 FDG PET/CT imaging for differentiating the lymph nodes between malignant lymphoma and benign lesions. Ann Nucl Med. 2013;27(2):163-9.
23. Miyake KK, Nakamoto Y, Togashi K. Dual-time-point 18F-FDG PET/CT in patients with colorectal cancer: clinical value of early delayed scanning. Ann Nucl Med. 2012;26(6):492-500.
24. Yamazaki M, Ideta T, Kudo S, Nakazawa M. Evaluation of artificial hip joint with radiofrequency heating issues during mri examination: a comparison between 1.5 T and 3 T. Nihon Hoshasen Gijutsu Gakkai Zasshi. 2016;72(6):480-8.